

ACCURACY OF AB INITIO TECHNIQUE IN PREDICTING THE STRUCTURAL, ELECTRONIC, MECHANICAL AND ELASTIC PROPERTIES OF RHODIUM AND RUTHENIUM.

Omamoke O. E. Enaroseha^{1*}, Godwin K. Agbajor¹, Obed Oyibo², Jude O. Vwavware³

¹Department of Physics, Delta State University, Abraka, Nigeria

²Department of Physics, Delta State University of Science and Technology, Ozoro, Nigeria.

³Department of Physics, Dennis Osadebay Univeristy, Asaba, Delta State, Nigeria

*Corresponding Author: enarosehaomamoke@gmail.com

*Department of Physics, Delta State University, Abraka, Nigeria

Abstract

The structural, thermodynamics, electronics and mechanical properties of Rhodium and Ruthenium transition metals are analyzed using the first principle calculations in this research. We adopted the DFT with the solution of Kohn – Sham equation given and using the Xcrysden package where the elemental structures were obtained and the PAW pseudo – potentials and GGA to treat the exchange – correlation function with the PBE functional.

The results for the lattice parameters deviated from experimental and theoretical results with approximately 1.6% for Ru and 1.9% for Rh. The bulk moduli agree with other reported results reported in the literature. The outcome of this investigation shows that the examined elements are mechanically stable as they agreed excellently with the results discussed in the literature. The band three – fold, two – fold degenerate. And non – degenerate levels are represented by the parameters for Rh and Ru respectively are C_{44} is 2.0 and 221, $C_{11} - C_{12}$ is 0.19 and 238, and $2C_{11} - 2C_{12}$ is 8.74 and 1376. The results also indicate that Ru exhibits anisotropic tendencies compared to Rh in terms of its elastic characteristics and more prone to modify its properties depending on the direction of its covalent bonding while Rh withstand breaking during experimental development compared to Ru because of its anisotropy's greater deviation from unity, hence, this is accurately given that it's also stiffer and tougher.

Keywords: Bulk moduli, Rhodium, Ruthenium, DFT, GGA

1.0 INTRODUCTION

The quest for the knowledge of individual relevant features of transition metals has motivated several researches to acquire credible information on these elements. To describe completely the quantum mechanical conduct in transition metals it is strictly necessary to calculate the many-electron wavefunction for the system. In principle this may be obtained from the time-independent Schrodinger equation [1], but in practice the potential experienced by each electron is dictated by the behaviour of all electrons in the solid [2,3,4]. Accordingly, Pan and his team carried research on rhodium (Rh) and some alloys using quasi – harmonic Debye model[5]. All ab initio calculations (total energy, elastic properties electron density distribution, etc.) of present work are based on 'Cambridge Serial Total Energy Package' (CASTEP) code and ultrasoft pseudopotential, together with the Perdew–Burke–Ernzerhof generalized gradient approximation exchange–correlation functions are applied. Plane-wave

basis set with energy cut-off 500.00 eV is applied for Rh, RhH, and RhH₂, respectively. Pseudoatomic calculations are performed for Rh 4d⁸ 5s¹, H 1s¹. From the study, the FCC at (0,0,0) of Rh atom engrossed all lattice points. In the work, lattice constants of Rh, RhH, and RhH₂ are 3.894, 4.076, and 4.383 Å, respectively, which agree with other experimental or theoretic data. Furthermore, it showed that Rh is mechanically stable under the condition of 0 GPa and 0–2000 K, 0 K and 0–100 GPa. The elastic constants and bulk modulus decrease with temperature and increase with pressure.

Also C_v of Rh, RhH, and RhH₂ as a function of temperature and pressure. The thermal expansion coefficient (α) of Rh, RhH, and RhH₂ were also investigated by some researchers[6].

They performed their calculations within the density functional theory (DFT) framework as implemented in the Cambridge Serial Total Energy Package (CASTEP) software. The electronic core interactions between nucleus and atoms were treated by the ultrasoft pseudopotentials. The exchange correlation functional was described by generalized gradient approximation (GGA) with the Perdew–Burke–Ernzerhof (PBE) functional form[7]. The electron wave function was expanded in a basis set of plane waves with a kinetic energy cutoff of 500 eV. The Brillouin zone integrations used Monkhorst–Pack grids of a 12 × 12 × 12 mesh. The structural relaxation was stopped until the total energy, the max force, and the max displacement were within 1×10^{-5} eV/atom, 0.03 eV/Å, and 0.001 Å, respectively. Furthermore, the properties of refractory metals Rh, and other metals have been systematically investigated using DFT[8]. All calculations performed in their work were carried out by the Vienna ab initio simulation package (VASP) using the first-principle method based on DFT. The projector augmented-wave method was applied to describe electronic interactions. The GGA proved to have a better result than the Local Density Approximation (LDA) to describe the exchange correlation energy of transitional metals by Domain. Hence, the GGA of the Perdew-Burke-Ernzerh (PBE) is adopted to treat exchange and correlation items in this study. In order to make the calculation result more accurate, after several attempts, the plane-wave cutoff energy of 520 eV is selected finally.

The interesting physical properties of Rhodium(Rh) and Ruthenium(Ru) and its effective usage in technological advancement has motivated us to study their structural, thermodynamic, electronic and mechanical properties for effective usage amongst other transition metals. Hence the specific objectives of the studies is to calculate: the structural properties of Rhodium and Ruthenium using Xcryden code, the electronic properties (band structure and density of state), the mechanical properties (ductility, plasticity, tensile stress and tensile strain) of Rhodium and Ruthenium using the elastic constant C_{11} , C_{12} , and C_{44} . and to determine the elastic properties of Rhodium and Ruthenium from DFT.

2.0 METHODOLOGY AND THEORETICAL OVERVIEW

To describe completely the quantum mechanical characteristics of electrons in solids it is strictly necessary to calculate the many-electron wave function for the system. In principle this may be obtained from the time-independent Schrodinger equation, but in practice the potential experienced by each electron is dictated by the behaviour of all electrons in the solid. Solving the Schrodinger equation directly for all these electrons would thus require us to solve a system

of around 10^{23} simultaneous differential equations. Such a calculation is preposterous for present-day computers, and is likely to remain so for the foreseeable future[9].

To apply the Schrödinger equation, write down the Hamiltonian for the system, accounting for the kinetic and potential energies of the particles constituting the system, then insert it into the Schrödinger equation. For a system of particles localized at different locations in the system, the wavefunctions become a function of their localization such that the equation 4 becomes:

$$H\psi(r_1, \dots, r_n) = E\psi(r_1, \dots, r_n) \quad (1)$$

where ψ is the many electron wave function, E is the system energy and H is the Hamiltonian of the system given by (in atomic units). Where the Hamiltonian is the sum of kinetic and potential energy terms of the system, this is given as:

$$H = T + V \quad (2)$$

The single electron of the hydrogen atom in a coulombic potentials for many body Hamiltonian is

$$H = -\frac{\hbar^2}{2m_e} \nabla_r^2 - \frac{e^2}{4\pi\epsilon_0 r} \quad (2)$$

Where \hbar is the reduced planks constant, m_e is electron mass and e is the Coulombic charge of the electron.

Thus we can write for a system of particles having N_e number of electrons and N_n number of nuclei, the Hamiltonian is given as:

$$H = T_e + V_{ne} + V_{ee} + V_{nn} \quad (3)$$

Where the terms have their meaning as: T_e : quantum kinetic energy of the electrons; V_{ee} : electron-electron interactions ; V_{nn} : electrostatic nucleus-nucleus repulsion ; V_{en} : electrostatic electron-nucleus attraction (electrons in the field of all the nuclei)

In general, we can rewrite the equation (4) as follows to include the individual terms :

$$H = -\frac{\hbar^2}{2m_e} \sum_i^{N_e} \nabla_i^2 + \frac{e^2}{4\pi\epsilon_0} \left[-\sum_i^{N_e} \sum_l^{N_n} \left(\frac{Z_l}{|r_1 - R_l|} \right) + \frac{1}{2} \sum_i^{N_e} \sum_{j \neq 1}^{N_e} \left(\frac{1}{|r_1 - r_j|} \right) + \frac{1}{2} \sum_l^{N_n} \sum_{j \neq 1}^{N_n} \left(\frac{Z_l Z_j}{|R_l - R_j|} \right) \right] \quad (4)$$

In solving the equation (4), several methods have been devised to find accurate approximations. There are two methods, wave – function-based and density – based and are further divided into different approaches.

2.1. Density functional theory (DFT)

The DFT treats the electron density as the central variable rather than the many-body wavefunction. Together, this implies that it refers to a function of electron density, which in itself is another function of three spatial variables [10]. An early density functional theory was proposed by Thomas and Fermi. This took the kinetic energy to be a functional of the electron density. In ground-state DFT, our interest is in systems of N interacting electrons described by the Hamiltonian

$$\hat{H} = \hat{T} + \hat{V} + \hat{V}_{ee} \quad (5)$$

$$E\psi = \left(-\sum_{i=1}^N \frac{\nabla_i^2}{2} + \sum_{i=1}^N v(r_i) + \frac{1}{2} \sum_{i=1}^N \sum_{i=j}^N \frac{1}{|r_i - r_j|} \right) \psi \quad (6)$$

with the kinetic, potential, and interaction energy operators \hat{T} , \hat{V} , and \hat{V}_{ee} , respectively. The foundations of density-functional theory are the Hohenberg–Kohn and Kohn–Sham theorems[11].

3.0 MATERIALS AND COMPUTATIONAL PROCEDURES

3.1 MATERIALS: The materials that aided us in the research are: Pseudopotentials, Laptop (Core i7), Rhodium and Rutherfordium, Quantum espresso package and other Packages in quantum espresso

3.2 COMPUTATIONAL PROCEDURES

The alatfm from the quantum espresso simulations are used as the cell dimension to obtain the band structure by running the following commands on the following scripts

(a) For band_down.in we use ;

`~/q-e-qe-6.7.0/bin/bands.x<band_down.in> band_down.out` to run the script:

```
&BANDS
prefix='Sc'
outdir='./'
filband='Sc_down'
spin_component=2
lsym=.true.
```

(b) For band_up.in we use ;

`~/q-e-qe-6.7.0/bin/bands.x<band_up.in> band_up.out` to run the script:

```
&BANDS
prefix='Sc'
outdir='./'
filband='Sc_down'
spin_component=2
lsym=.true.
```

(c) For Sc.band.in we use `~/q-e-qe-6.7.0/bin/pw.x<Sc.band.in> Sc.band.out` on the terminal to run the script below.

```
&control
calculation = 'bands',
prefix='Sc'
pseudo_dir='/home/nathaniel/pseudo/',
outdir='./',
/
&system
ibrav=2,
celldm(1)= 9.4588,
```

```

nat=1, ntyp=1,
nspin=2
starting_magnetization(1)= 0.5
starting_magnetization(2)= 0.5
starting_magnetization(3)= 0.5
occupations='smearing', smearing='mv', degauss=0.02,
ecutwfc=38.22, nbnd=10
/
&electrons
mixing_beta = 0.7
diagonalization='david'

```

4.0 RESULTS AND ANALYSIS

The calculated results obtained from the first principle consideration for the two transition elements Rhodium and Ruthenium using the DFT within the PBE generalized gradient approximation method as implemented in quantum espresso are presented and discussed in section 4.1 to section 4.4.

4.1 Structural Properties

Table 4.1: structural properties of Rhodium and Ruthenium

Properties		Rhodium	Ruthenium
a(A°)	Present work	5.69	3.62
	Other calculations	5.64 [12]	3.83 [12]
B(GPa)	Present work	3.00	304
	Other calculations	3.11 [12]	309[12]
B'(GPa)	Present work	12	7
	Other calculations	11[5]	9[5]
E _f (eV)	Present work	0.008	0.100
	Other calculations	0.009 [12]	0.107 [12]

We looked at the transition elements Rhodium and Ruthenium. They crystallize in the Fm3m structure with space group F432 as previously stated. To create the structure of the elements, the input file for each of these elements was uploaded into the Xcryden package.

Table 4.1 displays the results for the lattice parameter, bulk modulus, and pressure derivatives that were determined from the convergence of the lattice constant by fitting the computed results for a range of lattice parameters ($-0.3x + 0.3$) in steps of 0.1 (where x is an experimental lattice parameter value), fitted to the third order Birch-Murnaghan equation of state as given in the form[13]

$$E_v = E_0 + \frac{9BV_0}{16} \left\{ \left[\left(\frac{v_0}{v} \right)^{\frac{2}{3}} - 1 \right]^3 B' + \left[\left(\frac{v_0}{v} \right)^{\frac{2}{3}} - 1 \right]^2 \times \left[6 - 4 \left(\frac{v_0}{v} \right)^{2/3} \right] \right\} \quad (7)$$

In line with the pattern seen in [14], an increase in the molar mass of the 4d electron was found to increase the lattice constant of the compound. However, as all 4d electrons have the same atomic radius of 135 pm, this was not the case for the atomic radii. The lattice parameter result, which differs by roughly 1.5% for Ru and 1.8% for Rh from experimental and theoretical results. Both parts are consistent with earlier reports, it can be said. The bulk moduli also add up experiment data and other published findings.

The energy of formation must be negative, or the compound must be more stable than its component parts at absolute zero, for half – Heusler alloys[15] to be thermodynamically stable in their ground state. The equation below can be used to determine the formation energy for each alloy:

$$E_{formation} = E_{Mn} + E_Q + E_{Sb} \quad (8)$$

The fact that they have a negative energy of formation suggests that they are both easily synthesized in a laboratory and thermally stable.

4.2. Electronic properties

Table 4.2: The band gap of Rutherfordium and Rhodium

	Ru	Rh
Band Gap	0.0000	0.0000

The band structure and density of states were generated using the quantum espresso code and using the cell dimension obtained from the ferromagnetic state of the elements. The zero band gap indicates that these materials are indeed metals with conductivity. Their band structure is as shown in Fig. 4.1 and 4.2 below. The corresponding density of state shows a peak across the Fermi level indicating an engulfing of the covalent band over the valence band.

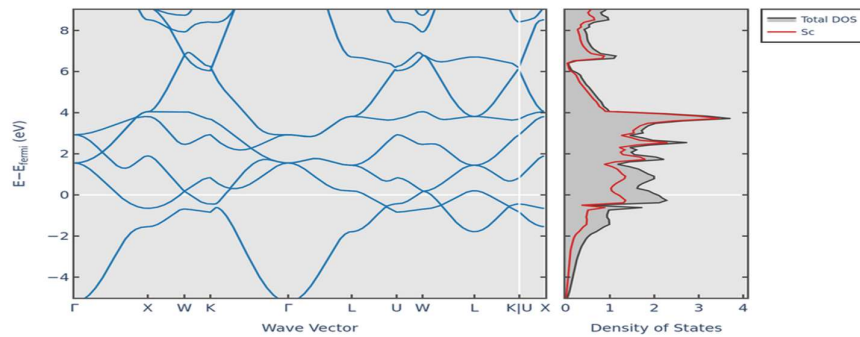


Figure 4.1: Band Structure and density of state of Ru

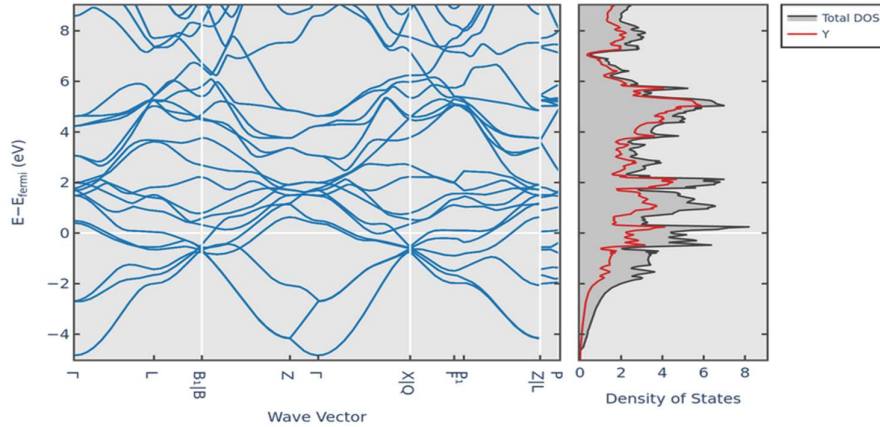


Figure 4.2: Band Structure and Density of state of Rh

4.3. Mechanical properties

Table 4.3: The mechanical properties of Rutherfordium and Rhodium

Properties		Rhodium	Ruthenium
C'		0.032	39.67
C ₁₁	Present work	2.29	450
	Other calculations	3.00 [5]	476 [5]
C ₁₂	Present work	2.10	212
	Other calculations	3.00 [5]	226 [5]
C ₄₄	Present work	2.00	221
	Other calculations	2.00 [5]	243 [5]
C ₁₁ - C ₁₂		0.19	
2C ₁₁ + 2C ₁₂		8.74	

The mechanical and dynamical behaviors of a crystal are connected by the solids' elastic constants, which also provide important details about the nature of forces in solids[16]. Elastic constants can be used to describe how materials flex when subjected to any tiny stresses. the impact of strain on a material's electrical characteristics. Three distinct elastic constants—C₁₁, C₁₂, and C₄₄—apply to cubic crystals. In order to determine the mechanical stability of the alloys under investigation, the elastic constants of the materials were examined, and the results are shown in Table 4.3. These elastic constants provide the criterion for the mechanical stability of the alloy. An alloy must have positive strain in order for it to be mechanically stable.

Results from this work therefore imply that the elements studied are mechanically stable which is in good agreement with literatures. The parameter C_{44} , $C_{11} - C_{12}$ and $2C_{11} + 2C_{12}$ represents the three fold, two-fold degenerate and non-degenerate levels of the bands in the cubic system.

4.4. Elastic properties

Table 4.4: Elastic properties of Rhodium and Rutherfordium

Properties		Rhodium	Ruthenium
G_v		1.213	148.470
G_R		0.00035	2.879
G	Present work	0.607	75.675
	Other calculations	0.992[12]	72.987[5]
B/G	Present work	4.942	4.017
	Other calculations	4.23[5]	4.441 [5,12]
E	Present work	1.706	389.9
	Other calculations	1.811[12]	380.25[12]
μ	Present work	0.405	0.286
	Other calculations	0.360[12]	0.301[5]
A	Present work	21.05	1.857
	Other calculations	8.71[5]	1.518[5]
H	Present work	0.030	0.068
	Other calculations	0.020[5]	0.068[5]

As shown in Table 4.4, the elastic properties of materials include the Shear Modulus, Anisotropy, Young's modulus, Poisson's ratio, and Hardness. These properties are derived from Hooke's law. Accordingly, the shear modulus's G_v and G_R , as well as the Voigt and Reuss approximation, were presented. The ratio of tensile stress to tensile strain, or the young's modulus E, represents how stiff a material is. All of the alloys' E values show a high level of stiffness, and they are in close agreement with experimental results. Therefore, Rh is both stiffer and harder than Ru.

The bulk modulus B, which measures how well a material can withstand fracture, to shear modulus G, which measures how well a material can withstand plastic deformations, is another elastic parameter that is shown. The ratio, commonly known as the Pugh's ratio, controls the material's ductile/brittle characteristic. During the production of materials, the ductile/brittle

behavior of the materials is crucial. B/G is important around 4.942, according to Bhardwaj and Singh's research. The material is ductile if $B/G > 4.942$; else, it is brittle.. According to the computed B/G values in table 4.4, both components are ductile.

Finally, since $H > 0.26$, the poisson's ratio, which predicts the potential bonding of the compound's atoms, supports ionic bonding for both Rh and Ru. Given that it is negative, the Cauchy pressure for Sc described by $C_{12} - C_{14}$ points to a directed covalent bonding. Anisotropic materials are direction dependant, whereas isotropic materials have qualities that are direction independent. In other terms, an anisotropic material is one that exhibits a directional divergence from unity. According to the findings, Rh exhibited anisotropic tendencies compared to Ru and is thus more prone to modify its properties depending on the direction of its covalent bonds. Additionally, we may say that it will withstand breaking during experimental development compared to Ru because of its anisotropy's greater deviation from unity.

5. 0 CONCLUSIONS

In order to use Rhodium and Ruthenium effectively in technological advancement, it is crucial to understand their properties. Consequently, numerous researchers have conducted a number of studies to determine these elements' structural, thermodynamic, electronic, optical, and mechanical characteristics. In order to improve production, hybridization, and doping (when necessary) with other elements in the periodic table, the first principle calculation was used in this work to determine the properties of these elements in the periodic table and checkmate the result with already known experimental properties of these elements. For the structural properties of these elements, the result for the lattice parameter which deviates from experimental and theoretical results with approximately 1.6% for Ru and 1.9% for Rh . Both elements can be said consistent with previous reports. The bulk moduli also tally experiments and other reported results.

Additionally, the cell dimension derived from the ferromagnetic state of the elements was used to construct the band structure and density of states for its electrical structure using the quantum espresso code[17]. These substances are in fact metals with conductivity, as indicated by the zero band gap. The structure of their band is as follows. A peak across the Fermi level may be seen in the corresponding density of states, suggesting that the covalent band has engulfed the valence band. The outcome of this investigation consequently suggests that the examined elements are mechanically stable in addition to its mechanical qualities, which is in excellent agreement with literature. The bands' three-fold, two-fold degenerate, and non-degenerate levels are represented by the parameters C_{44} , $C_{11} - C_{12}$, and $2C_{11} + 2C_{12}$.

The results also indicate that Ru show more anisotropic tendencies compared to Rh in terms of its elastic characteristics and is more prone to modify its properties depending on the direction of its covalent bonding. Additionally, we may say that it will withstand breaking during experimental development compared to Ru because of its anisotropy's greater deviation from unity. Of course, this is accurate given that it is also stiffer and tougher. We have also earlier employed the exact diagonalization techniques on some novel materials[18], Ab ignition on

AgGaS₂ and AgGaSe₂ [19] and also the inter – atomic force constant methods[20,21,22] to investigated Aluminium and Copper[20]; Nickel and Platinum[21], Lead and Palladium[22].

REFERENCES

- [1] Enaroseha O. E. Omamoke, Obed Oyibo, Oghenevovwero E. Esi, Edward O. Tuggen, and Jennifer A. Nomuoja . *European Chemical Bulletin* 12 (Special Issue 5), 290 – 297 (2023).. DOI: - 10.31838/ecb/2023.12.si5.034
- [2] Akash Singh and Yumeng Li. *Computational Materials Science* Vol. 227, 112272 – 112282, (2023).. doi [10.1016/j.commatsci.2023.112272](https://doi.org/10.1016/j.commatsci.2023.112272)
- [3] Wei Xie, Yu-Hao Liu, Xinwei Fan and Hai-Hu Wen . *Supercond. Sci. Technol.* Vol. 36, 075012 – 075024, (2023).. doi [10.1088/1361-6668/acd608](https://doi.org/10.1088/1361-6668/acd608)
- [4] Enaroseha O. E. Omamoke, Priscilla O. Osuhor, Obed Oyibo and Ernest O. Ojegu. *Solid State Technology*, Vol. 64 (2), 1984 – 1999, (2021). .
- [5] Pan, G., Hu, C., Zhou, P., Wang, F., Zheng, Z., and Liang, B. *Journal of Materials Research*, 29(12), 1334–1343, (2014).. doi:10.1557/jmr.2014.141
- [6] Chen, B. S., Zuo, C. Y., Wang, C., Guan, X. Y., and Li, Y. Z. *Journal of Superconductivity and Novel Magnetism*, 31(3), 799–803, (2017). . doi:10.1007/s10948-017-4253-8.
- [7] Enaroseha O. E. Omamoke , Godwin K. Agbajor, O. J, Vwavware, Akpoyibo Ogheneovo. *Eur. Chem. Bull.* 2023, 12(Regular Issue 1), 2772–2779, (2023)..
- [8] Sun Y., Parbin S., Singh P.K., and Fortram M. *Journal of Materials Research*, 29(12), 1334–1343, (2020).. doi:10.1557/jmr.2014.141
- [9] Stephen Jenkins (1994). The many body problem and density functional theory. University of Exeter. Retrieved from <http://newton.ex.ac.uk/research/qsystems/people/jenkins/mbody/mbody3.html>.
- [10] Rindt, C., and Gastra-Nedeia, S. (2015). *Modeling thermochemical reactions in thermal energy storage systems: Methods and Applications Woodhead Publishing Series in Energy. Advances in Thermal Energy Storage Systems*, 375–415. doi:10.1533/9781782420965.3.375.
- [11] Kurth, S., Marques, M. A. L., & Gross, E. K. U. (2005). Density-Functional Theory. *Encyclopedia of Condensed Matter Physics*, ed, by F. Bassani, J. Liedt, P. and Wyder (Elsevier) 395–402. doi:10.1016/b0-12-369401-9/00445-9
- [12] Zhou, Y., Yu, W., Khan, A., Chong, X., and Feng, J. *Journal of Micromechanics and Molecular Physics*, Vol. 5(2), 2030001, (2020).. doi:10.1142/s2424913020300017.
- [13] Hao L., K. Lei, H. Huang, L. Ye, S. Yang, H. Yu, M. Batmunkh, Y. Zhang and T. Ma (2019). Surface – Halogenation – Induced – Atomic – Site Activation and Local Charge Separation for Superb CO₂ Photo reduction *Advanced Materials* 31(25), 1900546 – 1900566.
- [14] Srikrishna Kandand Sbradhip P. (2018). Experimentation of First Principle Calculations of some metals and non metals. *Journal of Physics Series: Conference Series*, 1531, 012047
- [15] Enaroseha O. E. Omamoke, Priscilla O. Osuhor and Obed Oyibo . *The Journal of Applied Sciences Research*, 8 (1): 1 – 14, (2021).

- [16] Saini F., Simeon K. I., Mmadufi F.I. and Bethen I. O. (2014) Introduction to Many – Body Physics, Piers Coleman, Cambridge U. Press. Physics Today, 70(5), 59–60. doi:10.1063/pt.3.3558
- [17] Gionozzi P. *et. al* . QUANTUM ESPRESSO: a modular and open-source software project for quantum simulations of materials. J. Phys. Cond. Matter 21(39): 395502, (2009)
- [18] Enaroseha O. E. Omamoke, Obed Oyibo, and N. Okpara (2021). Analysis of Ground State Properties of Interacting Electrons in the Anderson Model. *The Journal of Applied Sciences Research*, 8(1), 15-27.
- [19] Omehe N. N. and Enaroseha O. E. Omamoke (2019) Ab INITIO INVESTIGATION OF AgGaS₂ and AgGaSe₂. *International Journal of Engineering Applied Sciences and Technology*, Vol. 4,(5), 354-360
- [20] Enaroseha O. E. Omamoke, Obed Oyibo, Priscilla O. Osuhor, and Ovie Oghenerhoro (2021) Lattice Dynamics in Some FCC Metals: Application of Phonon Dispersions in Nickel (Ni) and Platinum (Pt). *Solid State Technology*. Vol. 64 (2), 4640 – 4655.
- [21] Enaroseha O. E. Omamoke, Priscilla O. Osuhor, and Obed Oyibo (2021). Theoretical Study of Phonon Spectra in Aluminium (Al) and Copper (Cu): Application of Density Functional Theory and Inter – Atomic Force Constant. *Solid State Technology*. Vol. 64 (2), 1984 – 1999.
- [22]. Enaroseha O. E. Omamoke, Priscilla O. Osuhor and Obed Oyibo. (2021). Phonon Dispersion Relation of Lead (Pb) and Palladium (Pd). *The Journal of Applied Sciences Research*, 8(1), 1-14.